Bounded film evolution with nonlinear surface properties

By C. A. DEBISSCHOP[1]† ‡, R. J. BRAUN[1] ¶ AND S. A. SNOW[2]

[1]Department of Mathematical Sciences, University of Delaware, Newark, DE 19716, USA

[2]Dow Corning Corporation, Mail #C043C1, Midland, MI 48686-0994, USA

(Received 12 September 2001)

We study the evolution of a Newtonian free surface of a thin film above a solid wall. We consider the case in which the horizontal solid is covered by a non-wetting fluid and an insoluble monolayer of surfactant is present on the fluid-air interface. We pose a model that incorporates a variety of interfacial effects: van der Waals forces, variable surface tension and surface viscosity. The surface tension and surface viscosity depend nonlinearly on the surfactant concentration. Using lubrication theory we obtain a leading order description of the shape and velocity of the fluid-air interface, and the surfactant concentration, in the form of coupled nonlinear partial differential equations. A linear stability analysis reveals that the wavenumber that characterizes the marginal state is independent of the presence of the surfactant and the nonlinearity of the surface properties. We solve the 1+1-dimensional system numerically to obtain the spatio-temporal evolution of the free surface in the nonlinear regime, and observe the progression to rupture.

---

† Present address: Old Dominion Univ., Dept. of Mathematics and Statistics, Nofolk, VA.

‡ Supported by NSF Grant DMS-9631287.

¶ Supported by NSF Grant DMS-9631287 and Dow Corning Corporation Grant.

1. Introduction

We study the evolution of the free surface $h(x,t)$ of a thin Newtonian film oriented horizontally above a solid wall (see Figure 1). Air lies above the film, and an insoluble surfactant is present along the free surface.

The dynamics of the rupture of a thin film on a horizontal plate have been studied by a number of workers. Some review of the literature will be given here; for more comprehensive reviews, see Oron, Davis & Bankoff (1997) or Myers (1998). The linear theory for a thin film with air or a second viscous fluid above the film was studied by Jain & Ruckenstein (1976); they found that van der Waals forces caused rupture in either case for a thin enough film. They also studied the instability with and without an insoluble surfactant; they found that when the interface had a high concentration of surfactant, the rupture time was increased by a factor of four. The nonlinear stability of a thin film was studied by Williams & Davis (1982); in their work, van der Waals effects were included, but no surfactant was present. They developed a long wave evolution equation for the shape of the free surface of the film and found that for sufficiently long waves, the film would rupture. Their nonlinear results yielded a shorter time to rupture than the linear theory, and the rupture time depended strongly on the amplitude of the initial perturbation to the flat film surface. Sharma & Ruckenstein (1996) conducted a "finite amplitude instability" analysis; they concluded that the linear stability theory overestimated the effect of the average surface tension and underestimated the effect of surface viscosity, Marangoni effects, and van der Waals forces. Their analysis gave amplitude-dependent growth rate, wavelength, and rupture time. Nonlinear fits to the minimum film thickness and rupture time were computed by Hwang, Chang & Chen (1993); these fits allowed accurate prediction of the rupture time under certain conditions without solving the full nonlinear evolution problem.

These and other results have been extended in different ways. In some cases, more in-depth mathematical studies in three dimensions have led to insight into the rupture process for the isothermal film with van der Waals forces and no surfactant present. Three dimensional computations by Hwang, Lin & Uen (1997) showed that a film ruptures at a point, and not in a line as is computed in two dimensions. The three-dimensional point rupture occurred faster than the corresponding two-dimensional case. Similarity solutions near rupture were found by Zhang & Lister (1999) and Witelski & Bernoff (1999); they found a countably infinite set of profiles with only one being observed in dynamic computations. Witelski & Bernoff (2000) extended the analysis to three dimensions and found that line rupture in two dimensions and ring rupture in a cylindrical geometry are unstable to axisymmetric point rupture. When this instability is considered, the rupture time is less than that for restricted problems without the instability considered.

More physical effects have been added in some cases. Heat transfer and evaporation have been added to models of thin film evolution; for a review, see Oron, Davis & Bankoff (1997). The problem of the spreading of a surfactant on a thin liquid film has been studied; see, for example, Halpern, Jensen & Grotberg (1998), Williams & Jensen (2001), and the review by Grotberg (1994). The linear stability of a film, including thermal and solutal transport for a soluble surfactant, evaporation, Marangoni and interfacial viscous effects, as well as van der Waals forces, was studied by Danov *et al.* (1998); they examined the role of the various parameters in the linear theory. The nonlinear theory for the isothermal film with a soluble surfactant was studied by Lin, Hwang & Uen (2000). They compared several models (no surfactant, insoluble surfactant, Langmuir isotherm and a generalized Frumkin model) in two dimensions. They found that the soluble surfactant was generally destabilizing, in large part because the supply of surfactant from the bulk

mitigated the concentration gradients on the surface, thereby weakening the Marangoni effect. For the cases they studied the rupture process was driven by van der Waals forces.

Of particular interest is the paper by Edwards & Oron (1995); they studied the instability of a horizontal film on a plate with van der Waals forces and viscous interfacial stresses present. They obtained a set of two evolution equations for the film shape and the surface velocity; the surface concentration was not a dependent variable due to the assumption of weak Marangoni effects and/or strong surface diffusion of the surfactant. From the linear theory, they found that the effect of surface viscosity was to delay rupture; and that the cutoff wavenumber for instability was identical to the result of Williams & Davis (1982), independent of the surface viscosity. In the nonlinear theory, they found that the film did not rupture for nonzero surface viscosity, and that a small but finite-amplitude motion developed in the steady-state solutions at long time. The non-physical long-time behavior without rupture was thought to be due to the breakdown of the long wave approximation before rupture.

We develop a model that relaxes the assumptions used in Edwards & Oron (1995) in two ways. We allow the Marangoni effect to be strong and the surface diffusion to be sufficiently weak so that the transport of the insoluble surfactant must be considered in the evolution of the film. Secondly, we use a nonlinear equation of state for the surface tension of the air-film interface and variable surface viscosity that is representative of physical aqueous surfactant systems. Measurements for aqueous systems have recently been carried out by Lopez & Hirsa (1998,2000) and Vogel & Hirsa (2001), and we include these results in the model. Besides these measurements, nonlinear surface properties have been shown to have an impact on flows in the context of a drop in an extensional flow [Eggleton, Pawar & Stebe (1999)] and in a vertical draining free film [Naire, Braun & Snow (2001)]. In the vertical draining free film, the nonlinear surface properties showed

a marked localization of the flow in the surface compared to the case with a linear equation of state for the surface tension and a constant surface viscosity [Naire, Braun & Snow (2000)]. It is the contribution of the nonlinear surface properties that we wish to investigate in this context.

We formulate the problem in Section 2. A system of three nonlinear evolution equations for the film surface shape, the surfactant concentration on the surface, and the surface velocity is derived. The linear theory is studied in Section 3. Similar results to those of Edwards & Oron (1995) are found for the linear theory, except that the contribution of the Marangoni effect is explored, and the average surfactant concentration is a parameter even in the linear theory (because of the nonlinear surface properties). The nonlinear theory is investigated in Section 4 via numerical solution of the differential-algebraic system that results from spatial discretization. We determine that the film ruptures even in the presence of constant or variable surface viscosity; and localization of some of the dependent variables is particularly strong when the Marangoni effect is strong. Discussion of the results and a summary of conclusions follow in Sections 5 and 6, respectively.

2. Mathematical model

2.1. *Dimensional Formulation*

Our model is 1+1-dimensional: the height $\bar{h}$ of the free surface depends on the spatial position $\bar{x}$ and the time $\bar{t}$. The mean thickness $\bar{h}_0$ of the film is sufficiently small so that van der Waals forces are significant. We consider the evolution of the film over a wavelength L of a characteristic disturbance.

We describe the bulk fluid using the following conservation equations

$$\bar{\nabla} \cdot \bar{\mathbf{v}} = 0, \tag{2.1}$$

$$\rho\left(\frac{\partial\bar{\mathbf{v}}}{\partial\bar{t}}+\bar{\mathbf{v}}\cdot\bar{\nabla}\bar{\mathbf{v}}\right)=-\bar{\nabla}\bar{p}+\mu\bar{\nabla}^2\bar{\mathbf{v}}-\rho\bar{g}\mathbf{k}-\bar{\nabla}\bar{\phi}, \tag{2.2}$$

where the viscosity μ, the density ρ, and the gravitational acceleration $\bar{g}$ are constants, $\bar{p}$ is the pressure, $\bar{\mathbf{v}}=\bar{u}\mathbf{i}+\bar{w}\mathbf{k}$ is the velocity vector, and $\bar{\nabla}=\mathbf{i}\partial/\partial\bar{x}+\mathbf{k}\partial/\partial\bar{z}$ is the gradient operator. The Navier-Stokes equations (2.2) include a term involving the potential function $\bar{\phi}$, that represents van der Waals forces. The potential function has the form

$$\bar{\phi}=\hat{A}/(6\pi\bar{h}^3), \tag{2.3}$$

where $\hat{A}$ is the dimensional Hamaker constant.

The conservation equations are supplemented by no-slip and no-penetration conditions at the solid wall and by a kinematic condition at the free surface:

$$\bar{\mathbf{v}}=0 \quad \text{at} \quad \bar{z}=0, \tag{2.4}$$

$$\bar{w}=\bar{h}_{\bar{t}}+\bar{\mathbf{v}}\cdot\bar{\nabla}\bar{h} \quad \text{at} \quad \bar{z}=\bar{h}. \tag{2.5}$$

In addition at the free surface we use an interfacial stress condition

$$-\mathbf{n}\cdot\parallel\mathcal{T}\parallel=\bar{\nabla}_{\mathbf{s}}\cdot(\mathbf{I}_{\mathbf{s}}\bar{\sigma}+\tau^{\mathbf{s}}) \quad \text{at} \quad \bar{z}=\bar{h}, \tag{2.6}$$

that incorporates the Boussinesq-Scriven constitutive law

$$\tau^{\mathbf{s}}=(\kappa^{\mathbf{s}}-\mu^{\mathbf{s}})(\mathbf{I}_{\mathbf{s}}:\mathbf{D}_{\mathbf{s}})\mathbf{I}_{\mathbf{s}}+2\mu^{\mathbf{s}}\mathbf{D}_{\mathbf{s}}, \tag{2.7}$$

where $\mathbf{n}$ is the unit normal vector, $\bar{\sigma}$ is the surface tension, $\mathbf{I}$ is the spatial idemfactor, $\mathbf{I}_{\mathbf{s}}=\mathbf{I}-\mathbf{nn}$ is the surface idemfactor, $\bar{\nabla}_{\mathbf{s}}=\mathbf{I}_{\mathbf{s}}\cdot\bar{\nabla}$ is the surface gradient operator, and

$$\mathbf{D}_{\mathbf{s}}=\frac{(\bar{\nabla}_{\mathbf{s}}\bar{\mathbf{v}})\cdot\mathbf{I}_{\mathbf{s}}+\mathbf{I}_{\mathbf{s}}\cdot(\bar{\nabla}_{\mathbf{s}}\bar{\mathbf{v}})^T}{2}=(\bar{\nabla}_{\mathbf{s}}\cdot\bar{\mathbf{v}})\mathbf{I}_{\mathbf{s}} \tag{2.8}$$

is the surface rate of deformation tensor. The simplification in (2.8), the details of which are outlined in Naire (2000), applies in the 1+1-dimensional case. The normal and tangential components of the interfacial stress condition (2.6) are given by

$$-\mathbf{n}\cdot\parallel\mathcal{T}\parallel\cdot\mathbf{n}=2\mathcal{H}\bar{\sigma}+2\mathcal{H}(\kappa^{\mathbf{s}}+\mu^{\mathbf{s}})\bar{\nabla}_{\mathbf{s}}\cdot\bar{\mathbf{v}}, \tag{2.9}$$

$$-\mathbf{t}\cdot \parallel \mathcal{T} \parallel \cdot\mathbf{n} = \mathbf{t}\cdot\bar{\nabla}_{\mathbf{s}}\bar{\sigma} + (\kappa^{\mathbf{s}}+\mu^{\mathbf{s}})\mathbf{t}\cdot\bar{\nabla}_{\mathbf{s}}\bar{\nabla}_{\mathbf{s}}\cdot\bar{\mathbf{v}} + (\bar{\nabla}_{\mathbf{s}}\cdot\bar{\mathbf{v}})\mathbf{t}\cdot\bar{\nabla}_{\mathbf{s}}(\kappa^{\mathbf{s}}+\mu^{\mathbf{s}}), \quad (2.10)$$

where $\mathcal{H} = -\frac{1}{2}\bar{\nabla}_{\mathbf{s}}\cdot\mathbf{n}$ is the mean surface curvature, and $\mathbf{t}$ is the unit tangent vector. The first and last terms on the right-hand side of (2.10) appear because we consider variable, as opposed to constant, surface properties. We employ forms of the surface shear viscosity μ_s, the surface dilatational viscosity κ_s, and the surface tension $\bar{\sigma}$,

$$\mu^s = \mu^s_m G(\bar{\Gamma});\ \ \kappa^s \propto \mu^s, \quad (2.11)$$

$$\bar{\sigma}(\bar{\Gamma}) = \bar{\sigma}_m + \beta F(\bar{\Gamma});\ \ \bar{\sigma}_m = \bar{\sigma}(\bar{\Gamma}_m), \quad (2.12)$$

that depend nonlinearly on the surfactant concentration $\bar{\Gamma}$ (via the nonlinear functions F and G). We assume that the surface shear and dilatational viscosities are proportional. The subscript m denotes a reference quantity that may be chosen at or near where a phase change occurs, for example.

To close the model we include a transport equation at the free surface for an insoluble surfactant,

$$\bar{\Gamma}_t + \bar{\nabla}_s\cdot\left(\bar{\Gamma}\bar{\mathbf{v}}\right) = \bar{D}_s\bar{\nabla}_s^2\bar{\Gamma} \quad \text{at}\ \ \bar{z}=\bar{h}, \quad (2.13)$$

where $\bar{D}_s$ is the diffusion coefficient of the surfactant along the free surface. Since the surfactant that we consider strongly prefers the surface, a term that accounts for the flux of surfactant between the bulk and the free surface is absent from (2.13).

2.2. *Dimensionless Problem*

To nondimensionalize the model we introduce the following scales:

$$\begin{gathered}\bar{x} = xL,\ \ \bar{z} = z\bar{h}_0,\ \ \bar{t} = tL/U,\ \ \bar{u} = uU,\ \ \bar{w} = \epsilon wU,\\ \bar{h} = h\bar{h}_0,\ \ \bar{p} = p\hat{A}/\bar{h}_0^3,\ \ \bar{\phi} = \phi\hat{A}/\bar{h}_0^3,\ \ \bar{\sigma} = \sigma\bar{\sigma}_m,\ \ \bar{\Gamma} = \Gamma\bar{\Gamma}_m,\end{gathered} \quad (2.14)$$

where

$$U = \hat{A}/(\mu L\bar{h}_0),\ \ \epsilon = \bar{h}_0/L. \quad (2.15)$$

Upon substituting these quantities into the conservation equations we obtain, in component form,

$$\frac{\partial u}{\partial x} + \frac{\partial w}{\partial z} = 0, \tag{2.16}$$

$$\epsilon^3 \mathrm{Re}\left[\frac{\partial u}{\partial t} + u\frac{\partial u}{\partial x} + w\frac{\partial u}{\partial z}\right] = -\frac{\partial p}{\partial x} + \frac{\partial^2 u}{\partial z^2} + \epsilon^2\frac{\partial^2 u}{\partial x^2} - \frac{\partial \phi}{\partial x}, \tag{2.17}$$

$$\epsilon^5 \mathrm{Re}\left[\frac{\partial w}{\partial t} + u\frac{\partial w}{\partial x} + w\frac{\partial w}{\partial z}\right] = -\frac{\partial p}{\partial z} + \epsilon^2\frac{\partial^2 w}{\partial z^2} + \epsilon^4\frac{\partial^2 w}{\partial x^2} - \epsilon^4 \mathrm{St} - \frac{\partial \phi}{\partial z}, \tag{2.18}$$

where

$$\mathrm{Re} = \rho U L/(\epsilon\mu), \quad \mathrm{St} = \rho \bar{g} L^2/(\epsilon\mu).$$

The no-slip, no-penetration, and kinematic conditions become

$$u = w = 0 \quad \text{at} \quad z = 0, \tag{2.19}$$

$$w = \frac{\partial h}{\partial t} + u\frac{\partial h}{\partial x} \quad \text{at} \quad z = h. \tag{2.20}$$

In what follows, we employ nonlinear functions F and G of the form

$$F(\Gamma) = \tanh\left[\alpha_1(\gamma\Gamma - 1)\right] - \tanh\left[\alpha_1(\gamma - 1)\right],$$

$$G(\Gamma) = \exp(\alpha_2\Gamma) - 1,$$

where

$$\gamma = \bar{\Gamma}_m/\bar{\Gamma}_r,$$

and $\bar{\Gamma}_r$ is a reference quantity specific to the experimental data fit. We introduce the operator $\mathcal{D}$ for convenience,

$$\mathcal{D}f = \frac{\partial f}{\partial x} + h_x\frac{\partial f}{\partial z}, \tag{2.21}$$

and additional dimensionless parameters,

$$S = \frac{\epsilon\left(\kappa^s + \mu^s\right)_m}{\mu L}, \quad M = -\frac{\epsilon\gamma\alpha_1\beta}{\mu U}, \quad \mathrm{Ca} = \frac{\mu U}{\epsilon^3\bar{\sigma}_m}, \quad \mathrm{Pe} = \frac{UL}{\bar{D}_s}, \tag{2.22}$$

which are the so-called modified Boussinesq number, the Marangoni number, the Capillary number, and the Peclét number, respectively. We write the scaled tangential stress

condition as

$$N\left[2\epsilon^2 h_x\left(w_z-u_x\right)+\left(u_z+\epsilon^2 w_x\right)\left(1-\epsilon^2 h_x^2\right)\right]= \tag{2.23}$$

$$-M\dot{F}_\Gamma\Gamma_x+S\left[G\mathcal{D}\left(N^2\mathcal{D}u+N^2\epsilon^2 h_x\mathcal{D}w\right)+\right.$$

$$\left.\alpha_2 N^2 G_x\left(\mathcal{D}u+\epsilon^2 h_x\mathcal{D}w\right)\right] \quad \text{at} \quad z=h,$$

where

$$N\equiv\frac{1}{\sqrt{1+\epsilon^2 h_x^2}},\quad \dot{F}_\Gamma\equiv\frac{F_\Gamma}{\alpha_1}.$$

The nondimensional normal stress condition, likewise, has the form

$$-p+2\epsilon^2 N^2\left[\epsilon^2 h_x^2 u_x+w_z-h_x\left(u_z+\epsilon^2 w_x\right)\right]= \tag{2.24}$$

$$N^3 h_{xx}\left[\mathrm{Ca}^{-1}-\epsilon^2 MF(\Gamma)/\left(\gamma\alpha_1\right)+\epsilon^2 SGN^2\left(\mathcal{D}u+\epsilon^2 h_x\mathcal{D}w\right)\right] \quad \text{at} \quad z=h.$$

Finally, the scaled equation for the surfactant transport is

$$\Gamma_t+N^2\left[\mathcal{D}\left(\Gamma u\right)+\epsilon^2 h_x\mathcal{D}\left(\Gamma w\right)\right]= \tag{2.25}$$

$$\mathrm{Pe}^{-1}\left[\left(N^2\mathcal{D}\right)^2\Gamma+\left(\epsilon h_x N^2\mathcal{D}\right)^2\Gamma\right] \quad \text{at} \quad z=h.$$

3. Mathematical analysis

3.1. *Lubrication Theory*

The equilibrium film thickness $\bar{h}_0$ is small compared to the disturbance wavelength L, justifying a lubrication approximation. We expand the dependent variables regularly in $\epsilon=\bar{h}_0/L\ll 1$,

$$(u,w,p,\phi,h,\Gamma)=(u,w,p,\phi,h,\Gamma)^0+\epsilon(u,w,p,\phi,h,\Gamma)^1+\ldots, \tag{3.1}$$

and substitute these expansions into the dimensionless system (2.16)-(2.25), to obtain the leading order problem

$$u_x^0+w_z^0=0 \tag{3.2}$$

$$0 = -(p^0 + \phi^0)_x + u^0_{zz} \tag{3.3}$$

$$0 = -(p^0 + \phi^0)_z \tag{3.4}$$

$$u^0 = 0 \quad \text{at} \quad z = 0 \tag{3.5}$$

$$w^0 = 0 \quad \text{at} \quad z = 0 \tag{3.6}$$

$$w^0 = h^0_t + u^0 h^0_x \quad \text{at} \quad z = h^0 \tag{3.7}$$

$$u^0_z = -M\dot{F}_\Gamma(\Gamma^0)\Gamma^0{}_x + S\left[G\mathcal{D}^2 u^0 + \alpha_2 G_x \mathcal{D}u^0\right] \quad \text{at} \quad z = h^0 \tag{3.8}$$

$$-p^0 = \mathrm{Ca}^{-1} h^0_{xx} \quad \text{at} \quad z = h^0 \tag{3.9}$$

$$\Gamma^0_t + \mathcal{D}\left(\Gamma^0 u^0\right) = \mathrm{Pe}^{-1}\mathcal{D}^2\left(\Gamma^0\right) \quad \text{at} \quad z = h^0. \tag{3.10}$$

Equation (3.4) reveals that the sum of p^0 and ϕ^0 is independent of z. Thus, integration of Equation (3.3) with respect to z and use of (3.5),(3.9), lead to

$$u^0(x,z,t) = \frac{1}{2}\left[\phi^0_x - \mathrm{Ca}^{-1} h^0_{xxx}\right] z^2 + B(x,t)z, \tag{3.11}$$

where $B(x,t)$ is an arbitrary function. Substituting this expression for u^0 in (3.2), integrating the result with respect to z, and using condition (3.6), we obtain

$$w^0(x,z,t) = -\frac{1}{6}\left[\phi^0_x - \mathrm{Ca}^{-1} h^0_{xxx}\right] z^3 - \frac{1}{2} B_x z^2. \tag{3.12}$$

Next, we define the surface velocity as

$$u^{0(s)}(x,t) = u^0(x, h^0(x,t), t), \tag{3.13}$$

so that from (3.11) we have

$$B(x,t) = \frac{u^{0(s)}}{h^0} - \frac{1}{2}\left[\phi^0_x - \mathrm{Ca}^{-1} h^0_{xxx}\right] h^0. \tag{3.14}$$

In what follows we drop the superscripts that denote the leading order, for convenience. Substituting (3.11),(3.12) into the kinematic condition (3.7) and using (3.14), yields a

leading order equation for the evolution of the free surface,

$$h_t + \frac{1}{2}\left[hu^{(s)} - \frac{1}{6}h^3(\phi_x - \mathrm{Ca}^{-1}h_{xxx})\right]_x = 0. \tag{3.15}$$

Use of (3.11),(3.13),(3.14) in the tangential stress condition (3.8) produces a leading order equation for the surface velocity,

$$S\left[Gu_x^{(s)}\right]_x - \frac{u^{(s)}}{h} - \frac{1}{2}(\phi_x - \mathrm{Ca}^{-1}h_{xxx})h - M\dot{F}_\Gamma\Gamma_x = 0. \tag{3.16}$$

From the dimensional relation (2.3) together with the scaling for ϕ and h given in (2.14), the dimensionless relation for the potential function is

$$\phi = \frac{1}{6\pi h^3}. \tag{3.17}$$

Input of this specific form of ϕ into (3.15),(3.16) yields

$$h_t + \frac{1}{2}\left[hu^{(s)} + \frac{1}{6}\mathrm{Ca}^{-1}h^3h_{xxx} + \frac{1}{12\pi}\frac{h_x}{h}\right]_x = 0, \tag{3.18}$$

$$S\left[Gu_x^{(s)}\right]_x - \frac{u^{(s)}}{h} + \frac{1}{4\pi}\frac{h_x}{h^3} + \frac{1}{2}\mathrm{Ca}^{-1}hh_{xxx} - M\dot{F}_\Gamma\Gamma_x = 0. \tag{3.19}$$

Finally, using (3.11),(3.13) in (3.10) we obtain a leading order equation for the surfactant transport,

$$\Gamma_t + \left[\Gamma u^{(s)}\right]_x - \mathrm{Pe}^{-1}\Gamma_{xx} = 0. \tag{3.20}$$

3.2. *Linear Stability Analysis*

We seek the basic state, i.e., the time-independent solution of the leading order system (3.18)-(3.20). This steady state solution $(\hat{h}, \hat{u}^{(s)}, \hat{\Gamma})$, which we distinguish with a caret, satisfies

$$\left[\hat{h}\hat{u}^{(s)} - \frac{1}{6}\hat{h}^3(\phi_x - \mathrm{Ca}^{-1}\hat{h}_{xxx})\right]_x = 0, \tag{3.21}$$

$$S\left[G\hat{u}_x^{(s)}\right]_x - \frac{\hat{u}^{(s)}}{\hat{h}} - \frac{1}{2}(\phi_x - \mathrm{Ca}^{-1}\hat{h}_{xxx})\hat{h} - M\dot{F}_{\hat{\Gamma}}\hat{\Gamma}_x = 0, \tag{3.22}$$

$$\left[\hat{\Gamma}\hat{u}^{(s)}\right]_x - \mathrm{Pe}^{-1}\hat{\Gamma}_{xx} = 0. \tag{3.23}$$

One such steady solution is

$$\hat{h} = h_0, \quad \hat{u}^{(s)} = 0, \quad \hat{\Gamma} = \Gamma_{\text{ave}}, \tag{3.24}$$

where the average film thickness h_0 and the average surfactant concentration Γ_{ave} are constants. It would be interesting to examine the circumstances for which other steady solutions are possible as in Laugesen & Pugh (2000). Such a task is beyond the scope of this work.

The linear stability analysis is standard. We perturb the basic state using normal modes

$$\begin{aligned} h(x,t) &= \hat{h} + \tilde{H}\exp(\omega t + iqx), \\ \Gamma(x,t) &= \hat{\Gamma} + \tilde{\Gamma}\exp(\omega t + iqx), \\ u^{(s)}(x,t) &= \hat{u}^{(s)} + \tilde{u}^{(s)}\exp(\omega t + iqx), \end{aligned} \tag{3.25}$$

and substitute the perturbed quantities (3.25) into the time-dependent system (3.18)-(3.20). We expand the functions $\dot{F}_\Gamma$ and G as

$$\begin{aligned} \dot{F}_\Gamma(\Gamma) &= \dot{F}_\Gamma(\Gamma_{\text{ave}}) + \frac{1}{2}\dot{F}_{\Gamma\Gamma}(\Gamma_{\text{ave}})\tilde{\Gamma}\exp(\omega t + iqx) + \mathcal{O}(\tilde{\Gamma}^2), \\ G(\Gamma) &= G(\Gamma_{\text{ave}}) + \frac{1}{2}G_\Gamma(\Gamma_{\text{ave}})\tilde{\Gamma}\exp(\omega t + iqx) + \mathcal{O}(\tilde{\Gamma}^2), \end{aligned} \tag{3.26}$$

and obtain the linearized system $\boldsymbol{A}\vec{y} = \vec{0}$. Here $\vec{y} = \left[\tilde{H}, \tilde{u}^{(s)}, \tilde{\Gamma}\right]^T$ and

$$\boldsymbol{A} = \begin{bmatrix} \omega - q^2 V/(24\pi h_0) & \frac{1}{2}iqh_0 & 0 \\ iqV/(4\pi h_0^3) & -X/h_0 & -iqM\dot{F}_\Gamma(\Gamma_{\text{ave}}) \\ 0 & iq\text{Pe}\Gamma_{\text{ave}} & \omega\text{Pe} + q^2 \end{bmatrix}, \tag{3.27}$$

where

$$V \equiv V(q) = 1 - 2\pi\text{Ca}^{-1}h_0^4 q^2, \tag{3.28}$$

$$X \equiv X(q) = 1 + h_0 S G(\Gamma_{\text{ave}})q^2. \tag{3.29}$$

The existence of nontrivial solutions of the algebraic system requires that the determinant

of $\boldsymbol{A}$ is equal to zero. Imposing this condition yields the dispersion relation,

$$X\mathrm{Pe}\omega^2 + q^2\left[X + h_0 M\mathrm{Pe}\Gamma_{\mathrm{ave}}\dot{F}_\Gamma(\Gamma_{\mathrm{ave}}) - \mathrm{Pe}V(X+3)/(24\pi h_0)\right]\omega + \tag{3.30}$$
$$-q^4 V(X + 3 + h_0 M\mathrm{Pe}\Gamma_{\mathrm{ave}})/(24\pi h_0) = 0,$$

or, in explicit form,

$$\omega = \frac{q^2}{2X\mathrm{Pe}}\left\{-b + \sqrt{b^2 + \frac{\mathrm{Pe}}{6\pi h_0}VX\left[X + 3 + h_0 M\mathrm{Pe}\dot{F}_\Gamma(\Gamma_{\mathrm{ave}})\right]}\right\}, \tag{3.31}$$

where

$$b \equiv b(q) = X + h_0 M\mathrm{Pe}\dot{F}_\Gamma(\Gamma_{\mathrm{ave}}) - \frac{\mathrm{Pe}}{24\pi h_0}V(X+3).$$

We note that in the case $\mathrm{Pe} = 0$, we recover the dispersion relation presented in Edwards & Oron (1995), from Equation (3.30).

Upon setting $\omega = 0$ in (3.30), we most readily obtain the cutoff wavenumber, q_c,

$$q_c = \frac{1}{h_0^2}\sqrt{\frac{\mathrm{Ca}}{2\pi}}. \tag{3.32}$$

This result is identical to that of Williams & Davis (1982). Thus, in the linear regime, neither the presence of surfactant nor the nonlinearity of the surface properties influences the wavenumber that characterizes the marginal state.

The dominant mode satisfies $\partial\omega/\partial q = 0$. Performing implicit differentiation of (3.30) with respect to q^2 and setting $\partial\omega/\partial q^2 = 0$ in the result, we obtain a second relation for $\omega = \omega_m$ and $q = q_m$,

$$\mathrm{Pe}X_{q^2}\omega^2 + \left[q^2\left(X + h_0 M\mathrm{Pe}\Gamma_{\mathrm{ave}}\dot{F}_\Gamma(\Gamma_{\mathrm{ave}}) - \frac{\mathrm{Pe}}{24\pi h_0}V(X+3)\right)\right]_{q^2}\omega \tag{3.33}$$
$$-\left[\frac{q^4}{24\pi h_0}V(X + 3 + h_0 M\mathrm{Pe}\Gamma_{\mathrm{ave}}\dot{F}_\Gamma(\Gamma_{\mathrm{ave}}))\right]_{q^2} = 0.$$

Next, we multiply (3.30) by X_{q^2}, multiply (3.33) by X, and subtract the resulting relations, to obtain a relation linear in ω. Upon using the linear equation to substitute for $\omega = \omega_m$ in (3.30), we obtain a polynomial equation for $q = q_m$ that has degree sixteen!

To facilitate determination of the most dangerous mode, $q = q_m$, at this point we

make use of the reasoning of Edwards & Oron (1995). Because the effect of viscosity is a stabilizing one, the growth rate ω is the highest in the case of zero surface viscosity, i.e., when $S = 0$. This is demonstrated in Figure 2, which exhibits the the growth rate given by (3.31) for several values of S. In the limit of zero surface viscosity, the polynomial equation for q_m reduces to

$$a_1 q_m^6 + a_2 q_m^4 + a_3 q_m^2 + a_4 = 0, \tag{3.34}$$

where

$$a_1 = 16\pi^3 \mathrm{Pe}^2 h_0^{12},$$

$$a_2 = 2\pi^2 \mathrm{PeCa} h_0^8 (33\pi h_0^2 W - 48\pi h_0 - \mathrm{Pe}),$$

$$a_3 = 4\pi \mathrm{Ca}^2 h_0^4 (72\pi^2 h_0^3 W - 9\pi \mathrm{Pe} h_0^2 W + 18\pi h_0 \mathrm{Pe} + 2\mathrm{Pe}^2 - 38\pi^2 h_0^2 [1 - h_0^2 W^2]),$$

$$a_4 = \mathrm{Ca}^3 (6\pi \mathrm{Pe} h_0^2 W - 12\pi \mathrm{Pe} h_0 - 72\pi^2 \mathrm{Ca} h_0^3 W - \mathrm{Pe}^2 \mathrm{Ca} - 36\pi^2 \mathrm{Ca} h_0^2 [1 + h_0^2 W^2]),$$

and

$$W = M \mathrm{Pe} \Gamma_{\mathrm{ave}} \dot{F}_\Gamma(\Gamma_{\mathrm{ave}}). \tag{3.35}$$

Although we cannot solve this reduced equation exactly, certain limits provide useful information. Given zero surface viscosity, in the case of $\mathrm{Pe} = 0$ (and thus $W = 0$) we recover as the dominant mode the result of Williams & Davis (1982),

$$(q_m)_{WD} = \frac{1}{2h_0^2} \sqrt{\frac{\mathrm{Ca}}{\pi}}. \tag{3.36}$$

As shown in Figure 3, the dominant wavenumber does not deviate significantly from (3.36), for the values of the parameters that we employ.

A stronger Marangoni effect (e.g., for $M = 3700$) yields a deviation in the results as compared to (3.36) that is less than one percent. The Marangoni effect is also a stabilizing one, and the growth rate is the highest in its absence, i.e., when $M = 0$ (see Figure 4).

Given zero surface viscosity, in the case of $M = 0$ (and thus $W = 0$) with $\mathrm{Pe} \neq 0$,

we recover two roots: one is the dominant mode that is the result (3.36) of Williams & Davis (1982); the other root is the wavenumber $q = q_k$ associated with another critical point along the stability curve $\omega(q)$,

$$q_k = \frac{1}{h_0^2}\sqrt{\frac{\mathrm{Ca}}{2\pi}}\left[\sqrt{1+\frac{6\pi h_0}{\mathrm{Pe}}}\right]. \tag{3.37}$$

Although this point appears as a kink in Figure 2, we are not certain that there is in fact a jump in the slope there. This point is irrelevant in the context of instability, since the it exists where the growth rate ω is negative (see Figure 2). In the limit as $\mathrm{Pe} \to \infty$, the wavenumber given by (3.37) becomes the cutoff wavenumber (3.32).

4. Numerical results

Here we present and analyze results obtained from the numerical study of (3.18)-(3.20) for various limiting cases. Using centered finite differences we discretized the spatial derivatives. We then stepped the resulting differential-algebraic system in time using the DASSL solver [Brenan, Campbell & Petzold (1996)], with a meshsize of 5001 gridpoints. To maintain the symmetry expected in the solution we were forced to compute over half of the domain; the remaining half shown in each figure is a reflection of the computed solution. Where possible we compare with simpler theory. Where applicable, we use initial conditions for the film thickness and the surfactant concentration, having a perturbation to the basic state,

$$h(x,0) = 1 + \delta\cos(q_m x), \quad \Gamma(x,0) = \Gamma_{\mathrm{ave}}[1+\delta\cos(q_m x)], \quad \delta \ll 1, \tag{4.1}$$

where the dominant wavenumber that we employ,

$$q_m = \frac{1}{2}\sqrt{\frac{\mathrm{Ca}}{\pi}}, \tag{4.2}$$

is that obtained from the theory of Williams & Davis (1982). We make use of this result because it provides a good approximation for the values of the parameters we employ

(see Figure 3). Consistent with (4.1), we use the value $h_0 = 1$ to generate the results in this section.

We first consider the case of no Marangoni effect and zero surface viscosity (for definiteness we take $\Gamma = 0$). In the limit that the Marangoni number M and the Boussinesq number S are zero, we recover analytically the result of Williams & Davis (1982),

$$h_t + \left[\frac{1}{6\pi}\frac{h_x}{h} + \frac{1}{3\mathrm{Ca}}h^3 h_{xxx}\right]_x = 0. \tag{4.3}$$

This limit provided a means for us to test our three-equation code. Figure 5 demonstrates our computational result for $\mathrm{Ca} = 1.3$ in this limit, for a one percent perturbation ($\delta = 0.01$) to the basic state. The film thickness evolves to the Williams & Davis (1982) result at the end time, which is depicted by the set with the circles. The labels on the curves are dimensionless times, and rupture occurs nearly at $t = 1200$.

Next we consider the case of constant surface viscosity (i.e., constant $\kappa^{\mathbf{s}} + \mu^{\mathbf{s}}$) in the absence of the Marangoni effect. In the limit that the Marangoni number is zero, the surface viscosity is constant, and the surfactant concentration is unity, the three-equation system (3.18)-(3.20) reduces to two coupled nonlinear equations,

$$h_t + \frac{1}{2}\left[hu^{(s)} + \frac{1}{6\mathrm{Ca}}h^3 h_{xxx} + \frac{1}{12\pi}\frac{h_x}{h}\right]_x = 0 \tag{4.4}$$

$$Su^{(s)}_{xx} - \frac{u^s}{h} + \frac{1}{4\pi}\frac{h_x}{h^3} + \frac{1}{2\mathrm{Ca}}hh_{xxx} = 0. \tag{4.5}$$

To illustrate the effects of finite, yet constant, surface viscosity, we chose the parameters $\mathrm{Ca} = 1.3$, $S = 20$, which are representative of octanoic acid on a waxed surface [Ting *et al.* (1984)]. As expected, film rupture occurs. Figure 6 indicates that rupture occurs twice as slowly as in the case of zero viscosity, for this set of parameters. Initially the surface velocity evolves very slowly from its initial condition. When the film nears rupture, we see evolution on a fast scale. As depicted in Figure 7 the surface velocity curves are odd

about the spatial position where the film thickness reaches a minimum. In the trough, where destabilizing molecular forces dominate, the surface velocity is high.

In the absence of the Marangoni effect and given constant surface properties, as we increase the surface viscosity, rupture is delayed as expected. Figure 8 depicts the minimum film thickness as a function of time for several values of the Boussinesq number. Rupture is observed even for large values of the Boussinesq number, and there is a smooth departure from the result of Williams & Davis (1982).

In their work with other flows, Stebe and co-workers [Pawar & Stebe (1996); Eggleton, Pawar & Stebe (1999)] demonstrated that nonlinear surface properties are important. For virtually all physical materials the surface viscosity for a clean surface is negligible, and increases as the concentration of the surfactant increases. Indeed the surface tension decreases as the concentration of an insoluble surfactant increases. Lopez & Hirsa (1998) have measured the surface properties of an insoluble surfactant, hemicyanine in an air-water interface. We use their nonlinear correlations [Vogel & Hirsa (2001)] (see Figures 9-10), which they fit to data over a wide range of surfactant concentrations. We employ surfactant concentrations that range from a clean surface ($\Gamma = 0$) up to the value where a phase change occurs ($\Gamma = 1$).

Making use of the aforementioned correlations, we now illustrate the variable surface viscosity and the Marangoni effect numerically in the nonlinear regime. We use initial conditions for both the film thickness and the surfactant concentration, corresponding to a one percent perturbation ($\delta = 0.01$) to the basic state. We then calculate a consistent initial condition for the surface velocity from (3.19), using a tridiagonal solver.

Figures 11-19 exhibit the film thickness, the surface velocity, and the surfactant concentration profiles, for several values of time for three sets of parameters. The fixed parameters for these runs are Ca $= 1.7$, $S = 1.27$, $\Gamma_{\text{ave}} = 0.75$, and Pe $= 100$. The Marangoni

number and the Boussinesq number are as follows for the three cases we consider: A) $M = 1$, $S = 1.27$, B) $M = 1$, $S = 0$, and C) $M = 3700$, $S = 1.27$. In all cases film rupture is observed, as well as the slow-then-fast evolution of the surface velocity. As depicted for Case A (Figures 11-13), given nonzero surface viscosity and a weak Marangoni effect, the surface is not clean at the rupture point. The surface velocity is highest near the trough, and is sweeping surfactant out of the trough, but is not high enough to sweep it clean. The rupture is van der Waals driven. The inherent singularity in the surface velocity is mitigated by the surface viscosity to a high degree. That singularity is apparent in Case B (Figures 14-16), where surface viscosity is absent. The velocity exhibits a spike in the trough, and sweeps the trough clean of surfactant (Figure 15). The velocity data at the later times and certainly very close to the rupture time exhibit gridscale oscillation. We terminate the computation at $t = 4066$, before substantial gridscale oscillation has occurred. Given nonzero surface viscosity and a strong Marangoni effect, there is only a very slight decrease from the average value of the surfactant concentration at rupture, and the decrease is very localized. The velocity is the highest initially, as fluid moves from regions of low to high surface tension. Eventually the destabilizing van der Waals forces dominate and promote rupture. This is depicted in Case C (Figures 17-19). Based on the aforementioned cases, we can conclude that surface viscosity has a profound effect on the surfactant concentration profile.

The case of a strong Marangoni effect in the absence of surface viscosity (not shown) is hard to distinguish from Case C, according to data we computed for times such that the minimum film thickness $h(x,t)$ is less than 0.09. With the current formulation we had difficulty achieving convergence after such times. We cannot conclude much about what happens at the later times, but it appears that the surface velocity does not blow up and looks similar to that in Case C.

As the average surfactant concentration $\Gamma_{\text{ave}} \leq 0.75$ increases, we see delayed rupture times due to the Marangoni effect (see Figure 20). In fact, at $\Gamma_{\text{ave}} = 0.75$ we slightly exceed the fourfold increase in rupture time as predicted by the linear theory of Jain & Ruckenstein (1976) for high average surfactant concentration, on comparison with the Williams & Davis (1982) result (labeled as WD in Figure 20). We achieve a very slight bit above a fourfold increase due to the presence of a weak Marangoni effect. We see a decrease in the rupture time as Γ_{ave} increases above 0.75, due to the decrease in the surface tension gradient in the correlation (see Figure 9). Curve S in Figure 20 is a constant surface viscosity result ($S = 10$, $\Gamma = 1$) in the absence of the Marangoni effect (i.e., curve S is analogous to the curves in Figure 8, for Ca = 1.7). The value $S = 10$ used to generate curve S corresponds most closely to the value of the product $SG(\Gamma_{\text{ave}})$ for $\Gamma_{\text{ave}} = 1$, $S = 1.27$. Comparing curve S with the curve corresponding to $\Gamma_{\text{ave}} = 0.75$, we see that rupture is significantly delayed when the Marangoni effect is included. The Marangoni effect is dominating the contribution from the constant surface viscosity.

In Figure 21 curves S and WD are the constant viscosity and Williams & Davis (1982) results, respectively, mentioned previously; and the curves A, B, C correspond to the parameter sets mentioned previously. It is evident that the rupture time is most strongly delayed by the Marangoni effect and, to a lesser extent, by surface viscosity. In the case corresponding to curve C, we exceed the fourfold increase in rupture time as predicted by the linear theory of Jain & Ruckenstein (1976) for high average surfactant concentration, on comparison with the Williams & Davis (1982) result. We achieve a bit above a fourfold increase due to the presence of a strong Marangoni effect.

We now consider an alternative set of correlations for the nonlinear surface properties [Lopez & Hirsa (2000), Miraghaie & Lopez (2001)]. This correlation for the surface tension (Figure 22) is monotonic in the surfactant concentration Γ. Thus, as the average

surfactant concentration increases beyond 0.75, we continue to see delayed rupture times due to the Marangoni effect (see Figure 24). In Figure 24 curves S and WD are the constant viscosity and the Williams & Davis (1982) results, respectively, that correspond to the alternative correlations. We slightly exceed the fourfold increase in rupture time as predicted by the linear theory of Jain & Ruckenstein (1976) for high average surfactant concentration, on comparison with the Williams & Davis (1982) result (labeled as WD in Figure 24). We recall that we can achieve a slight bit above fourfold due to the presence of a weak Marangoni effect. Comparing curve S with the curve corresponding to $\Gamma_{\text{ave}} = 0.95$, we see that rupture again is significantly delayed when the Marangoni effect is included. For these parameters as well, the Marangoni effect is dominating the contribution from the constant surface viscosity.

5. Discussion

A hierarchy of cases were considered, beginning with a comparison with Williams & Davis (1982) for verification and continuing to a strong Marangoni effect case with van der Waals forces. The comparison with Williams & Davis (1982) verified the current approach and model. The addition of surface viscosity slowed down the rupture process, but for the cases we considered, the surface viscosity was not strong enough to effectively immobilize the surface. Thus, with surface viscous effects and no Marangoni effect, we did not observe as much as a factor of four in the increase of the rupture time, but we believe it would be obtained in the limit as S goes to infinity.

With a weak Marangoni effect added, the shear stresses generated by surface concentration gradients were not sufficient to qualitatively change the rupture process. The surfactant concentration was substantially lowered in the vicinity of rupture, but the area still retained a significant amount of surfactant at rupture.

When the strength of the Marangoni effect was increased, the initial disturbances in the concentration were effectively eliminated by the strong response to the concentration gradients; the perturbation in the free surface shape remained, however, and rupture still occurred. Near rupture there was a slight decrease in the concentration from its average value, that was quite localized; this lends some support to the approximation used in Edwards & Oron (1995). The regime in which they expected this behavior was for weak Marangoni effects and strong surface diffusion; we are able to achieve the nearly constant surfactant concentration with the opposite case where Marangoni effects are strong and surface diffusion is weak compared to advection (i.e., for large surface Peclét number).

The localization of the surfactant concentration is consistent with computations for vertical free films carried out by Naire *et al.* (2000,2001). The regions where gradients of surfactant concentration were significant remained localized near the top of the film for the cases they considered.

6. Summary

We have studied the linear and nonlinear stability of a thin film on a horizontal plate with an insoluble surfactant and interfacial viscous stresses. The model correctly finds that the film ruptures in the presence of both effects, and shows that the Marangoni and van der Waals forces can oppose each other to produce interesting dynamics. The films rupture in a line in this work; we can expect the instabilities of Zhang & Lister (1999) and Witelski & Bernoff (2000) to be present during the rupture process in this situation. The presence of the surfactant does not seem to have a particularly strong effect on the film thickness very near rupture in our model; however, the scaling of the surface velocity near rupture is abruptly changed by the introduction of surface viscosity. We are

currently investigating this behavior. In the early stages of the evolution, the Marangoni effect can strongly affect the evolution and the time to rupture.

REFERENCES

Brenan, K. E., Campbell, S. L. & Petzold, L. R. 1996 *Numerical Solution of Initial-Value Problems in Differential-Algebraic Equations.* Philadelphia: SIAM.

Danov, K. D., Alleborn, N., Raszillier, H. & Durst, F. 1998 The stability of evaporating thin liquid films in the presence of surfactant. I. Lubrication approximation and linear analysis. *Phys. Fluids* **10**, 131–143.

Edwards, D. A. & Oron, A. 1995 Instability of a non-wetting film with interfacial viscous stress. *J. Fluid Mech.* **298**, 287–309.

Eggleton, C. D., Pawar, Y. P. & Stebe, K. J. 1999 Insoluble surfactants on a drop in an extensional flow: a generalization of the stagnated surface limit to deforming interfaces. *J. Fluid Mech.* **385**, 79–99.

Grotberg, J. 1994 Pulmonary flow and transport phenomena. *Annu. Rev. Fluid Mech.* **26**, 529–571.

Halpern, D., Jensen, O. E. & Grotberg, J. B. 1998 A theoretical study of surfactant and liquid delivery into the lung. *J. Applied Physiology* **85**, 333–352.

Hwang, C.-C., Chang, S.-H. & Chen, J.-L. 1993 On the rupture process of thin liquid film. *J. Colloid Interface Sci.* **159**, 184–188.

Hwang, C.-C., Lin, C.-K. & Uen, W.-Y. 1997 A nonlinear three-dimensional rupture theory of thin liquid films. *J. Colloid Interface Sci.* **190**, 250–252.

Jain, R. K. & Ruckenstein, E. 1976 Stability of stagnant viscous films on a solid surface. *J. Colloid Interface Sci.* **54**, 108–116.

Laugesen, R. S. & Pugh, M. C. 2000 Linear stability of steady states for thin film and cahn-hilliard type equations. *Archives Ration. Mech. An.* **154**, 3–51.

Lin, C.-K., Hwang, C.-C., & Uen, W.-Y. 2000 Nonlinear rupture theory of thin liquid films with soluble surfactant. *J. Colloid Interface Sci.* **231**, 379–393.

Lopez, J. M. & Hirsa, A. 1998 Direct determination of the dependence of the surface shear and

dilatational viscosities on the thermodynamic state of the interface: theoretical foundations. *J. Colloid Interface Sci.* **206**, 231–239.

Lopez, J. M. & Hirsa, A. H. 2000 Surfactant-influenced gas-liquid interfaces: nonlinear equation of state and finite surface viscosities. *J. Colloid Interface Sci.* **229**, 575–583.

Miraghaie, R. & Hirsa, A. H. 2001 Private communication.

Myers, T. G. 1998 Thin films with high surface tension. *SIAM Rev.* **40**, 441–462.

Naire, S. 2000 Gravitationally-driven drainage of thin films. Ph.D. thesis, University of Delaware.

Naire, S., Braun, R. J. & Snow, S. A. 2000 An insoluble surfactant model for a vertical draining free film. *J. Colloid Interface Sci.* **230**, 91–106.

Naire, S., Braun, R. J. & Snow, S. A. 2001 An insoluble surfactant model for a vertical draining free film with variable surface viscosity. *Phys. Fluids*, to appear.

Oron, A., Davis, S. H. & Bankoff, S. G. 1997 Long-scale evolution of thin liquid films. *Rev. Mod. Phys.* **69**, 931–980.

Pawar, Y. & Stebe, K. J. 1996 Marangoni effects on drop deformation in an extensional flow: the role of surfactant physical chemistry. I. Insoluble surfactants. *Phys. Fluids* **8**, 1738–1751.

Sharma, A. & Ruckenstein, E. 1986 An analytical nonlinear theory of thin film rupture and its application to wetting films. *J. Colloid Interface Sci.* **113**, 456–479.

Ting, L., Wasan, D. T., Miyano, K. & Zu, S. Q. 1984 Longitudinal surface waves for the study of dynamic properties of surfactant systems I. Gas-liquid interface *J. Colloid Interface Sci.* **102**, 248–253.

Vogel, M. J. & Hirsa, A. H. 2001 Concentration measurements downstream of an insoluble monolayer front *J. Fluid Mech.*, submitted for publication.

Williams, M. B. & Davis, S. H. 1982 Nonlinear theory of film rupture. *J. Colloid Interface Sci.* **90**, 220–228.

Williams, H. A. R. & Jensen, O. E. 2001 Two-dimensional nonlinear advection-diffusion in a model of surfactant spreading on a thin liquid film. *IMA J. Appl. Math.* **66**, 55–82.

WITELSKI, T. P. & BERNOFF, A. J. 1999 Stability of self-similar solutions for van der waals driven thin film rupture. *Phys. Fluids* **11**, 2442–2445.

WITELSKI, T. P. & BERNOFF, A. J. 2000 Dynamics of three-dimensional thin film rupture. *Physica D* **147**, 155–176.

ZHANG, W. W. & LISTER, J. R. 1999 Similarity solutions for van der Waals rupture of a thin film on a solid substrate. *Phys. Fluids* **11**, 2454–2462.

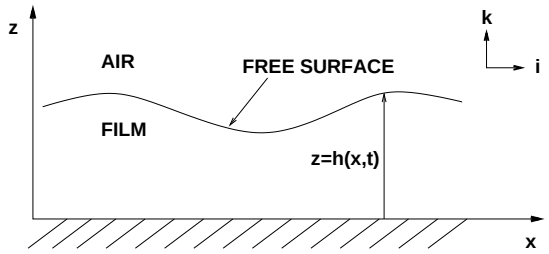

FIGURE 1. Schematic of the dimensionless physical system.

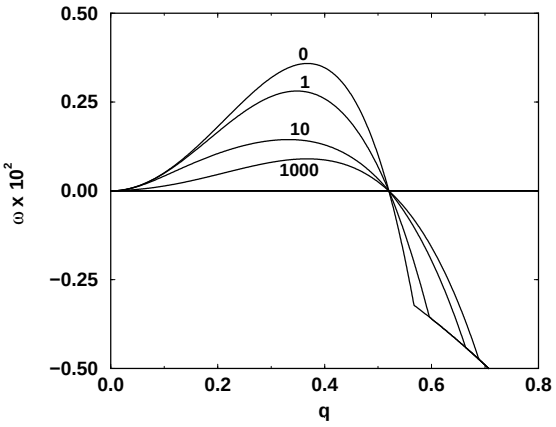

FIGURE 2. Growth rate versus wavenumber for several values of the Boussinesq number S, for variable surface viscosity and no Marangoni effect ($M = 0$, $\Gamma_{\text{ave}} = 0.75$, Ca $= 1.7$, Pe $= 100$, $h_0 = 1$).

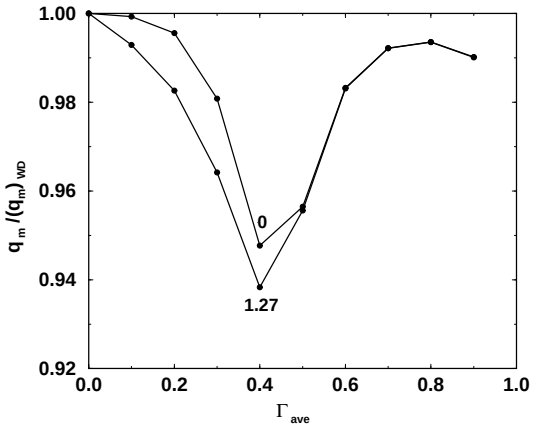

FIGURE 3. Ratio of actual dominant wavenumber to that predicted by Williams & Davis (1982), versus average surfactant concentration, for two values of the Boussinesq number S and with Marangoni effects ($M = 1$, Ca $= 1.7$, Pe $= 100$, $h_0 = 1$).

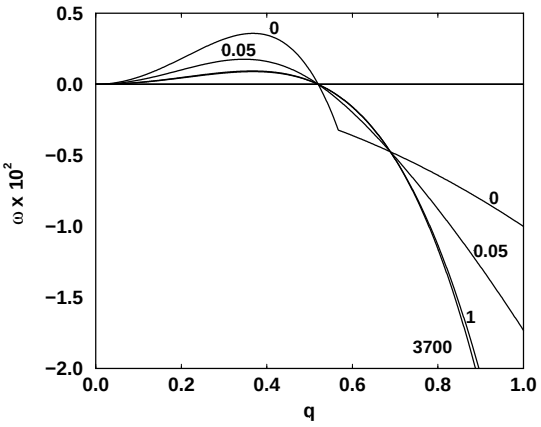

FIGURE 4. Growth rate versus wavenumber for several values of the Marangoni number M, in the absence of surface viscosity ($S = 0$, $\Gamma_{\text{ave}} = 0.75$, $\text{Ca} = 1.7$, $\text{Pe} = 100$, $h_0 = 1$).

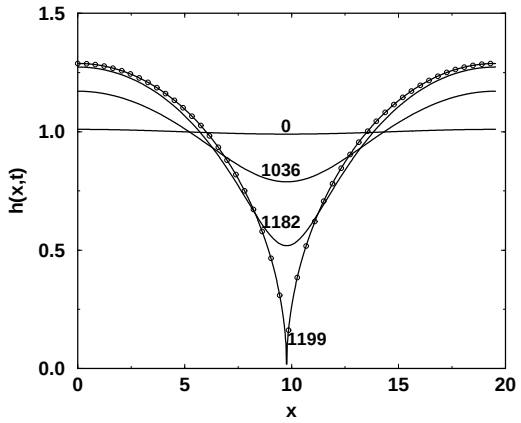

FIGURE 5. Film thickness versus spatial position for several values of time, in the absence of the Marangoni effect and surface viscosity ($M = S = 0$, $\Gamma = 0$, $\mathrm{Ca} = 1.3$). The final state is the Williams & Davis (1982) result, depicted by the set with the circles.

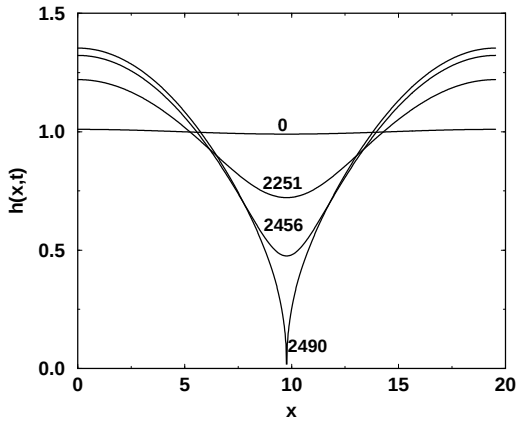

FIGURE 6. Film thickness versus spatial position for several values of time, for constant surface viscosity and no Marangoni effect ($M = 0$, $\Gamma = 1$, $\mathrm{Ca} = 1.3$, $S = 20$).

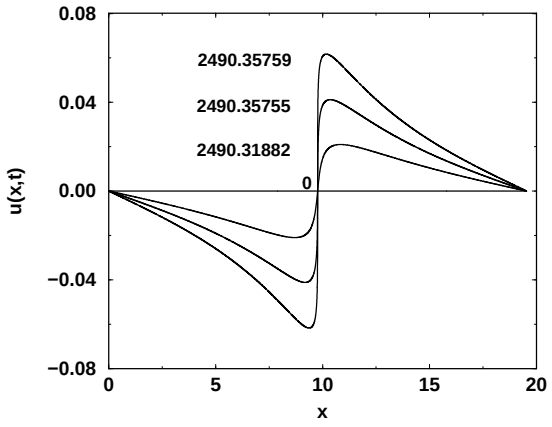

FIGURE 7. Surface velocity versus spatial position for several values of time ($M = 0$, $\Gamma = 1$, $\mathrm{Ca} = 1.3$, $S = 20$).

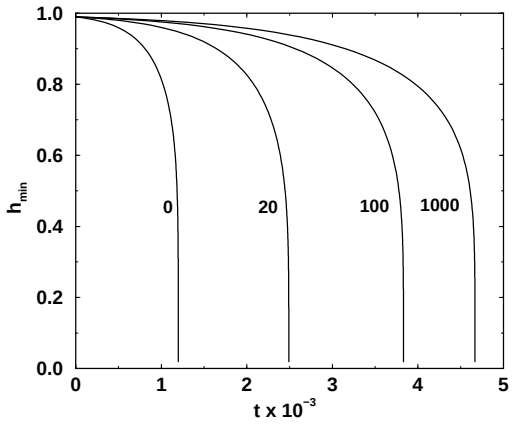

FIGURE 8. Minimum film thickness versus time for several values of the Boussinesq number S, for constant surface viscosity and no Marangoni effect ($M = 0$, $\Gamma = 1$, $\mathrm{Ca} = 1.3$).

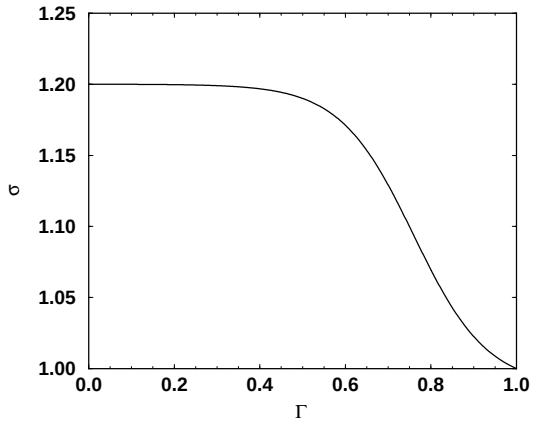

FIGURE 9. Nonlinear correlation of the surface tension as a function of the surfactant concentration, for hemicyanine in water ($\alpha_1 = -4.4$, $\bar{\Gamma}_m = 1.013718$ mg/m^2, $\bar{\Gamma}_r = 0.77$ mg/m^2, $\beta = 6.4$ dynes/cm, $\bar{\sigma}_r = 65.9$ dynes/cm, $\bar{\sigma}_m = \bar{\sigma}_r + \beta \tanh[\alpha_1(\gamma - 1)]$ [Vogel & Hirsa (2001)]).

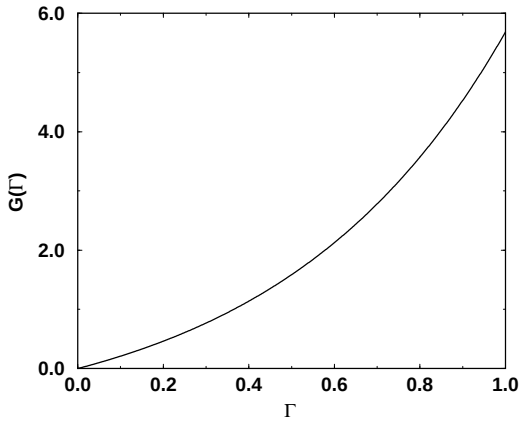

FIGURE 10. Nonlinear correlation of the surface viscosity as a function of the surfactant concentration, for hemicyanine in water ($\alpha_2 = 1.9$ [Miraghaie & Hirsa (2001)]).

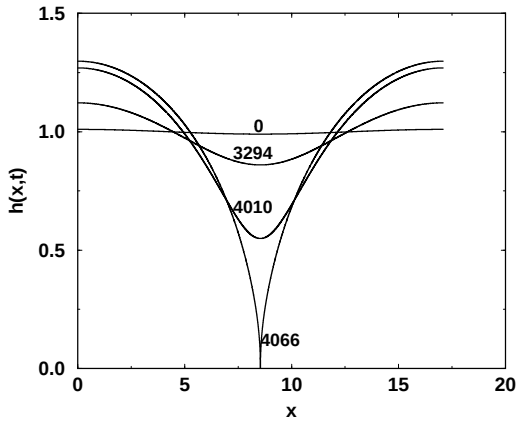

FIGURE 11. Film thickness versus spatial position for several values of time, for variable surface viscosity and with the Marangoni effect ($M = 1$, $\Gamma_{\rm ave} = 0.75$, Ca $= 1.7$, $S = 1.27$, Pe $= 100$).

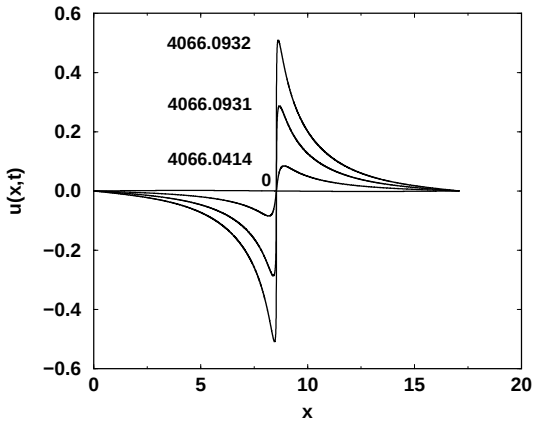

FIGURE 12. Surface velocity versus spatial position for several values of time ($M = 1$, $\Gamma_{\text{ave}} = 0.75$, Ca $= 1.7$, $S = 1.27$, Pe $= 100$).

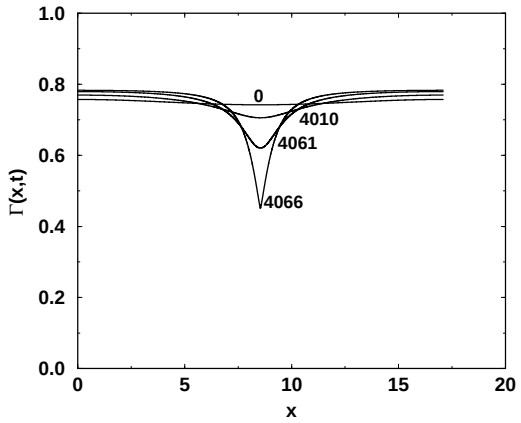

FIGURE 13. Surfactant concentration versus spatial position for several values of time ($M = 1$, $\Gamma_{\text{ave}} = 0.75$, Ca $= 1.7$, $S = 1.27$, Pe $= 100$).

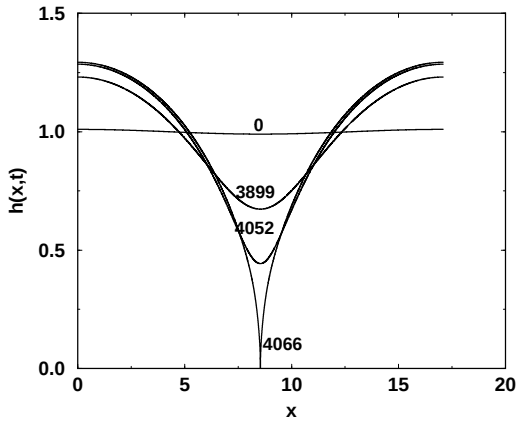

FIGURE 14. Film thickness versus spatial position for several values of time, with the Marangoni effect and no surface viscosity ($M = 1$, $\Gamma_{\text{ave}} = 0.75$, Ca $= 1.7$, $S = 0$, Pe $= 100$).

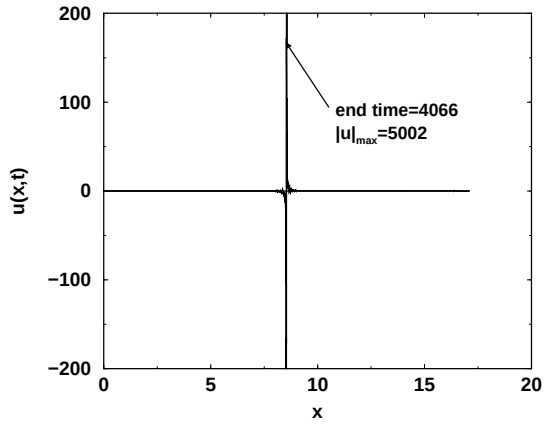

FIGURE 15. Surface velocity versus spatial position for several values of time ($M = 1$, $\Gamma_{\rm ave} = 0.75$, Ca $= 1.7$, $S = 0$, Pe $= 100$). The computation terminated at $t = 4066$ with $|u|_{\rm max} = 5002$ (not shown).

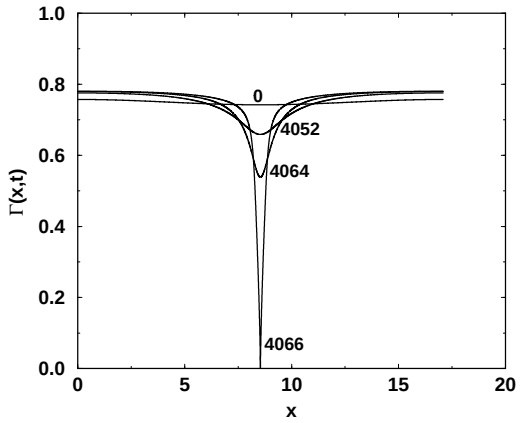

FIGURE 16. Surfactant concentration versus spatial position for several values of time ($M = 1$, $\Gamma_{\text{ave}} = 0.75$, Ca $= 1.7$, $S = 0$, Pe $= 100$).

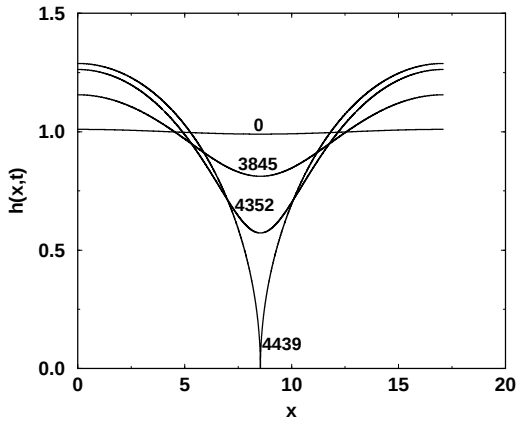

FIGURE 17. Film thickness versus spatial position for several values of time, for variable surface viscosity and with the Marangoni effect ($M = 3700$, $\Gamma_{\text{ave}} = 0.75$, $\text{Ca} = 1.7$, $S = 1.27$, $\text{Pe} = 100$).

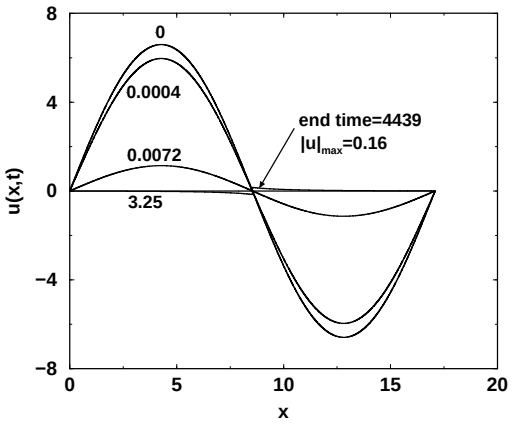

FIGURE 18. Surface velocity versus spatial position for several values of time ($M = 3700$, $\Gamma_{\text{ave}} = 0.75$, Ca $= 1.7$, $S = 1.27$, Pe $= 100$).

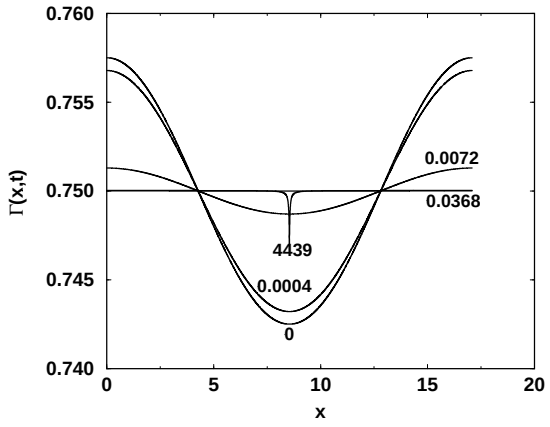

FIGURE 19. Surfactant concentration versus spatial position for several values of time ($M = 3700$, $\Gamma_{\text{ave}} = 0.75$, Ca $= 1.7$, $S = 1.27$, Pe $= 100$).

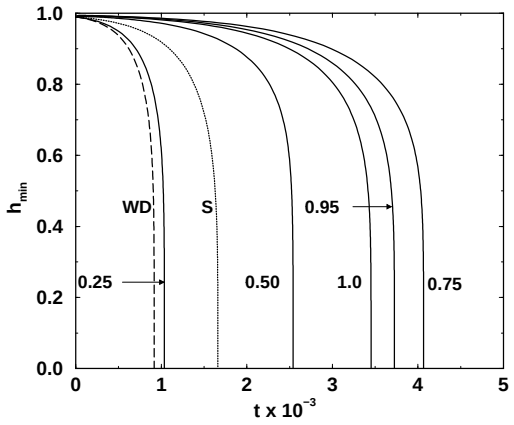

FIGURE 20. Minimum film thickness versus time for several values of the average surfactant concentration Γ_{ave}, for variable surface properties and with the Marangoni effect ($M = 1$, Ca $= 1.7$, $S = 1.27$, Pe $= 100$). Here, curve WD denotes the Williams & Davis (1982) result ($M = S = 0$, $\Gamma = 0$, Ca $= 1.7$). Curve S denotes a result for constant surface viscosity in the absence of the Marangoni effect ($M = 0$, $\Gamma = 1$, Ca $= 1.7$, $S = 10$).

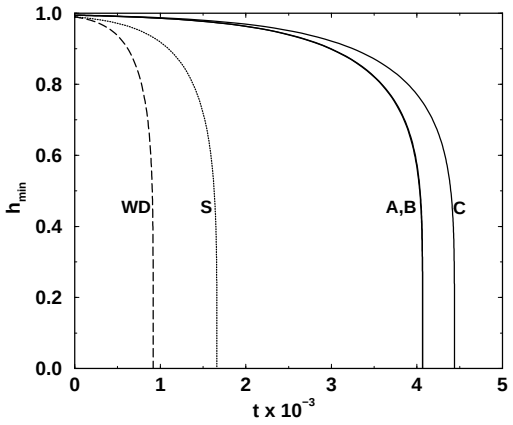

FIGURE 21. Minimum film thickness versus time for two values of the Marangoni number M and the Boussinesq number S, for variable surface properties and with the Marangoni effect (Ca = 1.7, Pe = 100, $\Gamma_{\rm ave}$ = 0.75). The labels correspond to the following parameters: A) $M = 1$, $S = 1.27$; B) $M = 1$, $S = 0$; C) $M = 3700$, $S = 1.27$. Here, curve WD denotes the Williams & Davis (1982) result ($M = S = 0$, $\Gamma = 0$, Ca = 1.7). Curve S denotes a result for constant surface viscosity in the absence of the Marangoni effect ($M = 0$, $\Gamma = 1$, Ca = 1.7, $S = 10$).

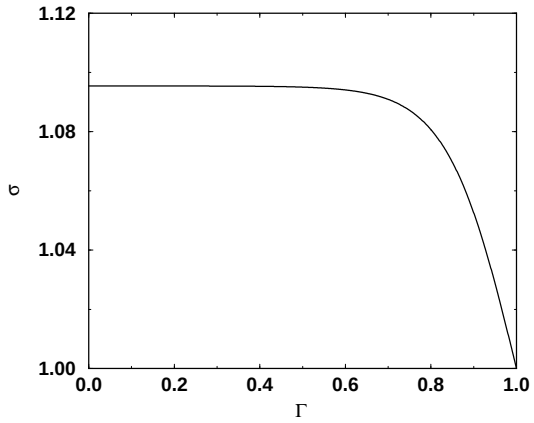

FIGURE 22. Nonlinear correlation of the surface tension as a function of the surfactant concentration, $\sigma = 1 + (\beta/\bar{\sigma}_m)\tanh\left[\alpha_1(\Gamma - 1)\right]$ ($\alpha_1 = -6.2$, $\beta = 6.4$ dynes/cm, $\bar{\sigma}_m = 66.2$ dynes/cm [Lopez & Hirsa (2000)]).

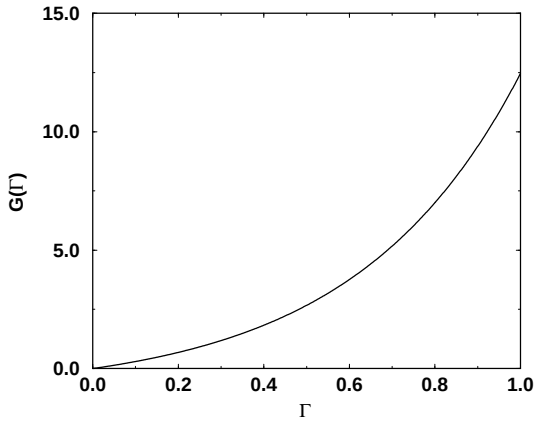

FIGURE 23. Nonlinear correlation of the surface viscosity as a function of the surfactant concentration ($\alpha_2 = 2.6$, $(\kappa^s + \mu^s)_m = 1.27 \times 10^{-3}$ g/s [Lopez & Hirsa (2000)]).

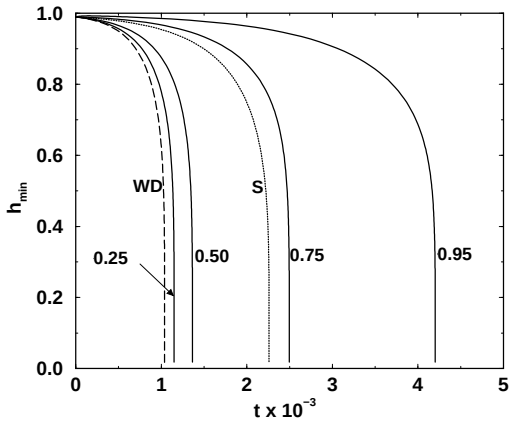

FIGURE 24. Minimum film thickness versus time for several values of the average surfactant concentration Γ_{ave}, for variable surface properties and with the Marangoni effect ($M = 0.4$, Ca $= 1.5$, $S = 1.27$, Pe $= 100$). Here, curve WD denotes the Williams & Davis (1982) result ($M = S = 0$, $\Gamma = 0$, Ca $= 1.5$). Curve S denotes a result for constant surface viscosity in the absence of the Marangoni effect ($M = 0$, $\Gamma = 1$, Ca $= 1.5$, $S = 20$).